

## STRESS AND MICROSTRUCTURE IN LPCVD POLYCRYSTALLINE SILICON FILMS: EXPERIMENTAL RESULTS AND CLOSED FORM MODELING OF STRESSES

P. KRULEVITCH<sup>†</sup>, G.C. JOHNSON<sup>†</sup>, and R.T. HOWE<sup>\*</sup>

<sup>†</sup>Berkeley Sensor & Actuator Center, Department of Mechanical Engineering

<sup>\*</sup>Berkeley Sensor & Actuator Center, Department of Electrical Engineering and Computer Sciences  
University of California, Berkeley, CA 94720

### ABSTRACT

Characterization of undoped polycrystalline silicon films indicates that correlations exist between stress and microstructure. Films of thickness between 0.5-3.6  $\mu\text{m}$  were deposited onto  $\text{SiO}_2$ -covered single crystal silicon wafers between 605 and 700°C using low pressure chemical vapor deposition (LPCVD). The average in-plane film stress and the stress gradient through the film thickness were determined from wafer curvature measurements, and film microstructure was studied with cross-sectional TEM. Films deposited near 605°C exhibit overall tensile stresses that result from an amorphous to crystalline phase change. At deposition temperatures exceeding 630°C, a columnar grain structure evolves out of a transition region of small grains at the  $\text{SiO}_2$  interface. The columnar films are compressive, with the source of compression linked to the region of small grains. Stress is modeled using a closed form solution that considers a linearly elastic contracting ellipsoidal inclusion near the surface of a half space. Several applications of the stress model are discussed.

### 1.0 INTRODUCTION

The newly developing field of micro-electro-mechanical systems (MEMS) employs micron scale thin film members that are totally or partially freed from the substrate. Upon release, the large stresses typically present in thin films often cause device failure by instability, curling, or fracture. In addition, stress affects device performance by, for example, altering the response of resonant microstructures [1] and thin film diaphragms [2]. Polycrystalline silicon (polysilicon) is commonly used for MEMS, and is the thin film considered here. The origin of large tensile and compressive intrinsic stresses is discussed in relation to the evolution of the polysilicon microstructure. Undoped polysilicon films deposited by low pressure chemical vapor deposition (LPCVD) near 600°C consist of more or less equi-axed grains and are tensile, due to an amorphous to crystalline solid state transformation that occurs during the film deposition. At deposition temperatures exceeding 630°C, the grains are columnar and the stress is compressive. The source of compression is still uncertain, but is shown to be related to a transition layer of small grains at the film/substrate interface.

Stress in the tensile films is modeled using a closed form solution by Seo and Mura [3] for a uniformly contracting ellipsoidal inclusion near the surface of a half space. By making the ellipsoid's axis normal to the surface very small relative to the other axes, the ellipsoid resembles a contracting film on top of a semi-infinite substrate. The advantage of a closed form solution is the ease with which parameters can be changed to model other situations. Reducing the ellipsoid to a sphere, the problem models an equi-axed grain near the film surface that has crystallized out of an amorphous region. In this case, the stress field in the single grain is found to be tri-axial. Seo and Mura's solution can be used to model other cases of stress in thin films, such as thermal stress, and some further applications of the model are discussed.

### 2.0 EXPERIMENTAL PROCEDURES

The experimental procedures for the polysilicon deposition and stress measurement have been published in detail elsewhere [4, 5], and a summary follows.

#### 2.1 Polysilicon Deposition

Polysilicon films 0.5-3.6  $\mu\text{m}$  thick were deposited by LPCVD from pure silane ( $\text{SiH}_4$ ). Four inch (111) or (100) single crystal silicon wafers coated with 100 nm thermal oxide served as substrates for all polysilicon films. The LPCVD processing parameters varied as follows: deposition temperature from 605-700°C, silane pressure from 300-550 mTorr, silane flow rate from 100-250 sccm, and deposition time from 30 to 150 minutes. Experimental runs were made for 26 different combinations of these variables. All measurements were made on the as-deposited undoped polysilicon films.

#### 2.2 Stress Measurement

The average in-plane film stress was calculated from wafer curvature, typically on six wafers per run. After measuring the curvature using an ultrasonic flatgage, the film was chemically removed from the polished side of the wafer and the curvature measurement repeated. The radius of curvature due to stress in the removed film,  $R_c$ , was determined from the difference between the two measurements, and the in-plane stress was calculated using Stoney's equation [6]

$$\sigma_{rr} = \frac{E_s L^2}{6(1 - v_s) t_f R_c} . \quad (1)$$

The subscripts *s* and *f* in Eq. (1) refer to substrate and film, *E* and *v* are Young's modulus and Poisson's ratio, respectively, and *t* is thickness. The estimated uncertainty in  $\sigma_{rr}$  is on the order of 10%.

By removing successive film layers using reactive ion etching in a  $\text{CCl}_4\text{-O}_2$  plasma and measuring the resulting changes in wafer curvature, the stress profile through the film thickness was determined. The average in-plane stress in each layer was found from Eq. (1), using the change in curvature before and after removing the layer to determine  $R_c$ . To confirm the accuracy of the stress profiling technique, the average film stress was calculated in two ways: (1) by averaging the stress in all the layers, and (2) by using the total curvature change before and after removing the entire film. These two values never differed by more than 7%.

### 2.3 Electron Microscopy

Cross-sectional TEM specimens were prepared by mechanically thinning the sample to about 30  $\mu\text{m}$  then ion-beam milling in a cold stage at 5 kV, as described in reference [7]. Specimens were examined in a Philips EM301 operating at 100 kV.

## 3.0 RESULTS AND DISCUSSION

Stress in the polysilicon films varies considerably with process conditions, as shown by Fig. 1, a plot of stress vs. deposition temperature for all experimental runs. Each diamond in Fig. 1 represents the average stress of six films from the same run. Asterisks denote "transition runs" in which the stress changes from tensile to compressive with wafer position in the boat (see [4, 5]). Depositions at 605°C produce tensile films, while films deposited between 630 and 700°C are compressive, with the magnitude of compression decreasing with increasing temperature.

### 3.1 Tensile Films

Fig. 2 shows two cross-sectional TEM micrographs of a tensile polysilicon film deposited at 605°C, with 2(A) showing a region at the upper surface of the film and 2(B) showing the entire film, including the 100 nm oxide layer. LPCVD silicon films deposited near the crystallization temperature ( $\approx 600^\circ\text{C}$ ) are known to initially form an amorphous film that subsequently crystallizes in the reactor [8-10]. Such an amorphous region is visible near the surface

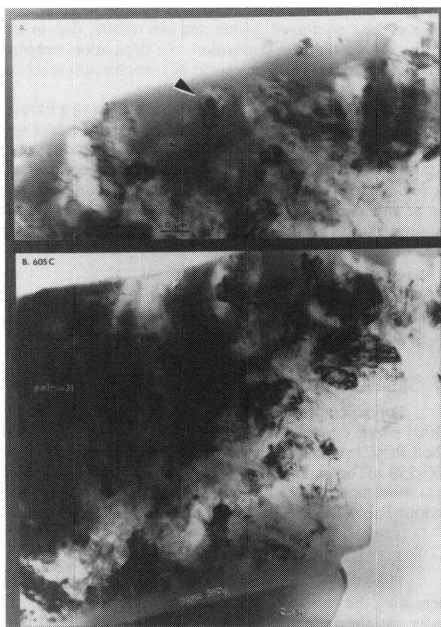
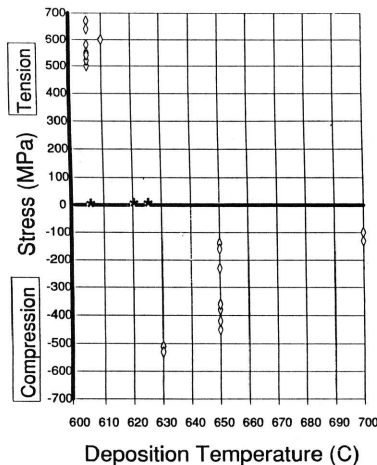


Figure 2. Cross-sectional TEM micrographs of a tensile film deposited at 605°C. 2(A) shows a region near the surface of the film in 2(B). A new grain, indicated by an arrow in 2(A), is just beginning to crystallize out of an amorphous region at the film surface.

Figure 1. Polysilicon film stress vs. deposition temperature for all experimental runs. Values are average stresses from six wafers per run. Asterisks indicate transition runs, in which stress varies from tensile to compressive with wafer position in the boat.

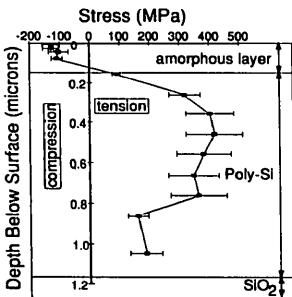


Figure 3. Stress profile of a tensile polysilicon film. The top amorphous layer is compressive, while crystalline layers are tensile.

center a distance  $z = c$  below the surface of a half space defined by  $z > 0$ . In this problem, both the inclusion and half space have the same isotropic elastic moduli. If freed from its matrix, the inclusion would contract (or expand) by a uniform dilatational strain (eigenstrain)  $\epsilon^*$ , but because it is perfectly bonded to the matrix, stresses are generated. By making the ellipse axis that is normal to the half space surface very small ( $a_3 \ll a_1 = a_2$ ), the inclusion resembles a thin film on top of an infinitely thick substrate. Furthermore, reducing the ellipse to a sphere ( $a_1 = a_2 = a_3 = a$ ), the problem models stress in a grain that has crystallized out of an amorphous region near the film surface, such as the one shown in Fig. 2(A). In this case, Seo and Mura's solution reduces to that given earlier by Mindlin and Cheng [13] in which the normal stresses inside the inclusion at  $r = 0$  are

$$\sigma_{rr} = \sigma_{\theta\theta} = \frac{2\mu\epsilon^*(1+v)a^3}{3(1-v)} \left\{ \frac{-2}{a^3} + \frac{(3+4v)}{(z+c)^3} - \frac{6z}{(z+c)^4} \right\} \quad (2)$$

$$\sigma_{zz} = \frac{2\mu\epsilon^*(1+v)a^3}{3(1-v)} \left\{ \frac{-2}{a^3} + \frac{2}{(z+c)^3} + \frac{12z}{(z+c)^4} \right\}$$

where  $\mu = E/(2(1+v))$  is the shear modulus of the inclusion and half space. The normal stresses outside the inclusion at  $r = 0$  are

$$\sigma_{rr} = \sigma_{\theta\theta} = \frac{2\mu\epsilon^*(1+v)a^3}{3(1-v)} \left\{ \frac{1}{(z-c)^3} + \frac{(3+4v)}{(z+c)^3} - \frac{6z}{(z+c)^4} \right\} \quad (3)$$

$$\sigma_{zz} = \frac{2\mu\epsilon^*(1+v)a^3}{3(1-v)} \left\{ \frac{-2}{(z-c)^3} + \frac{2}{(z+c)^3} \right\}.$$

The moduli for polysilicon are taken to be  $E = 170$  GPa [1],  $v = 0.25$ , and  $\mu = 68$  GPa. In addition, the transformation strain,  $\epsilon^*$ , must be specified. Janai *et al.* [14] measured the thickness change in amorphous atmospheric pressure CVD silicon films that occurred after a crystallizing anneal, and found an average strain in the  $z$ -direction of  $0.015 \pm 0.01$ . Assuming that in an unconstrained amorphous film (no substrate) a transformation strain  $\epsilon^*$  would result upon crystallization such that  $\epsilon_{zz} = \epsilon_{rr} = \epsilon_{\theta\theta} = \epsilon^*$ , then the observed thickness strain for the constrained film,  $\hat{\epsilon}_{zz}$ , is given by

$$\hat{\epsilon}_{zz} = \epsilon^* + 2v\epsilon^*. \quad (4)$$

From Eq. (4) with  $\hat{\epsilon}_{zz} = -1.5\%$  and  $v = 0.25$ , the isotropic transformation strain  $\epsilon^*$  is  $-1\%$  [5].

Fig. 4 shows the normal stresses  $\sigma_{rr}$  and  $\sigma_{zz}$  as a function of depth through the center of a thin ellipsoidal inclusion at the surface of a half space. Stress in the plane of the inclusion,  $\sigma_{rr}$ , is 2.3 GPa in the "film" and negligible in the "substrate", while the stress in the direction normal to the "film" is negligible everywhere. Shear stress  $\sigma_{rz}$  and normal stress  $\sigma_{zz}$  at the center of a "film" with  $a_1 = a_2 = 10^3 a_3$  are shown in Fig. 5 as a function of radial position. Both are negligible at the middle of the ellipse and increase rapidly at the edges. The radial stress predicted by the model,  $\sigma_{rr} = 2.3$  GPa, exceeds the experimental results by a factor of 3-4. However, when the additional

<sup>†</sup> Seo and Mura's solution contains a typographical error. In Eq.'s (10) and (11), the expression for  $\Delta$  should be:

$$\Delta = \sqrt{(a_1^2 + s)(a_2^2 + s)(a_3^2 + s)}$$

component of stress due to compression in the amorphous state ( $\approx -900$  MPa [12]) is added to the result, the new radial stress of 1.4 GPa is more reasonable. The two main sources of error in this analysis are in  $\epsilon^*$ , which has an uncertainty of  $\pm 70\%$ , and in the assumption of elastic deformations. At the temperature of deposition ( $T = 0.4T_m$ ), stresses on the order of 500 MPa may cause plastic deformation, resulting in stress relaxation. The fact that the stress decreases near the  $\text{SiO}_2$  layer (Fig. 3) indicates that stress relaxation may occur in the polysilicon films.

Stress in an equi-axed grain that has crystallized out of an amorphous region at the film surface, such as the one shown in Fig. 2(A), can be modeled using a spherical inclusion that is tangent to  $z = 0$  of the half space. Fig. 6 shows  $\sigma_{rr}$  and  $\sigma_{zz}$  as a function of depth through the center of such an inclusion 0.1  $\mu\text{m}$  in diameter. The in-plane stress,  $\sigma_{rr}$ , is actually compressive near the surface. Comparing with Fig. 3, the crystallization volume contraction may also contribute to compression in the first layers of the tensile polysilicon films.  $\sigma_{rr}$  becomes tensile just below the surface and reaches a value near 1.5 GPa at a depth of about 1/4 of the inclusion diameter. The out-of-plane stress,  $\sigma_{zz}$ , must be zero at the surface; however, it increases with depth, approaching  $\sigma_{rr}$  in magnitude. Thus, a newly crystallized grain surrounded by amorphous silicon is in a state of tri-axial stress. It is interesting to note that when the center of the inclusion is 1.5 diameters below the half space surface, the normal stresses  $\sigma_{rr}$  and  $\sigma_{zz}$  are within 1% of Eshelby's solution for a spherical inclusion in an infinite body [15].

### 3.3 Compressive Films

Films deposited at temperatures exceeding 630°C are compressive and have an entirely different microstructure [16], consisting of columnar grains that grow out of a transition region of small grains at the  $\text{SiO}_2$  interface. Fig. 7 presents cross-sectional TEM micrographs of compressive films deposited at 620, 650, and 700°C, which show that the thickness of the transition layer decreases with increasing deposition temperature.

The compressive intrinsic stress in these films appears to be related to this layer of small grains. The magnitude of the compressive stress decreases with increasing temperature (see Fig. 1), and by 700°C, where the transition layer of small grains has completely disappeared, the stress is on the order of the thermal stress (see section 3.4). Fig. 8, a stress profile through the thickness of a compressive film deposited at 650°C, shows that the compression is greatest near the  $\text{SiO}_2$  interface in the layer of small grains, and decreases in magnitude away from the substrate as the grains become columnar. Stress in the topmost film layers is also on the order of the thermal stress. The proposition that the compression is largest in the region of small grains also explains why the average compressive stress decreases with increasing film thickness, as shown in Fig. 9, a plot of stress vs. as-deposited film thickness for seven different runs at 650°C.

The actual cause of compression is still uncertain. One possible explanation concerns the evolution of the film microstructure. Columnar grains are formed through the process of grain growth competition [17], in which the initial distribution of grain orientations is random, but only those grains preferentially aligned with their direction of fastest growth parallel to the film normal continue to grow, at the expense of inclined grains. There is a high driving force for growth in one direction ((110) for films deposited between 630 and 650°C, and (100) for 700°C depositions [4]) in the polysilicon films. Thus, an incoming atom may still deposit itself in the grain boundary region between an inclined grain and a more vertical one. Even though this will cause an increase in the strain energy, it may be the lowest overall energy state for the atom. This explanation accounts for the large stresses in the transition region of small inclined grains, and the decrease in stress as the grains become more vertical away from the substrate (Fig. 8). Another argument as to the source of compression in the polysilicon films is based on the densities of amorphous and crystalline silicon [18]. Void-free amorphous silicon is actually expected to expand upon

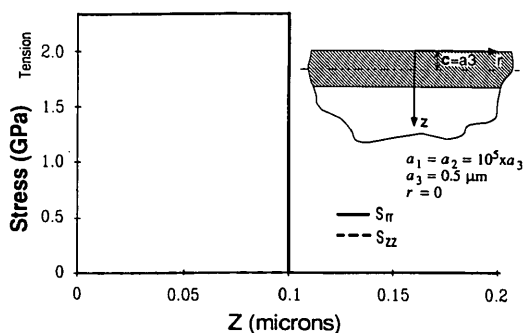


Figure 4.  $\sigma_{rr}$  and  $\sigma_{zz}$  vs. depth for disc-shaped uniformly contracting inclusion that is tangent to the half space surface. The problem models stress in a contracting polysilicon film on a single crystal silicon substrate. The radial stress is large and constant in the "film" but negligible in the "substrate."  $\sigma_{zz}$  is negligible everywhere.

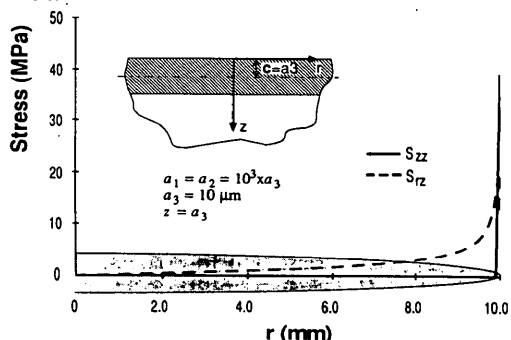


Figure 5. Shear stress  $\sigma_{zz}$  and normal stress  $\sigma_{rr}$  vs. radial position  $r$  for the same case as Fig. 4.

crystallization [19, 20] because the diamond cubic structure has a very low atomic packing density of 34%, compared to 74% for face centered cubic. At deposition temperatures near 605°C, the amorphous silicon surface layer may contain pores, causing contraction upon crystallization and resulting in tensile stress; however, the compressive films, deposited at higher temperatures, have an entirely different microstructure and crystallization process. One possible source of compression could be the result of newly deposited silicon atoms briefly forming a void-free amorphous solid, then expanding when joining the crystalline film. Once the columnar microstructure has evolved, adatoms can immediately add to the fast growing crystalline planes without inducing any compression, which is consistent with the stress profile in Fig. 8.

### 3.4 Additional Applications of Stress Model

The solution for an ellipse in a half space is easily modified to model other problems of stress in thin films. Thermal stress can be modeled using the problem considered in section 3.2 with  $a_1 = a_2 = a_3 = 10^5 \times a_3$ , but setting the

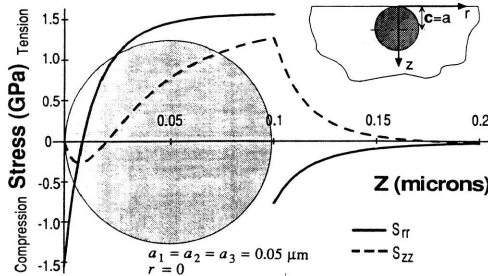


Figure 6. Normal stresses  $\sigma_{rr}$  and  $\sigma_{zz}$  vs. depth through the center of a uniformly contracting spherical inclusion that is tangent to the surface of a half space. The sphere models a polysilicon grain that has undergone an amorphous to crystalline transformation.

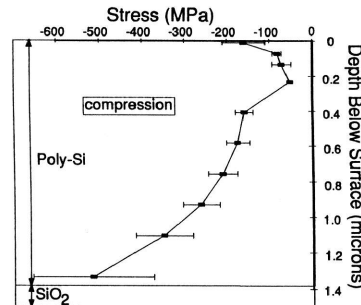
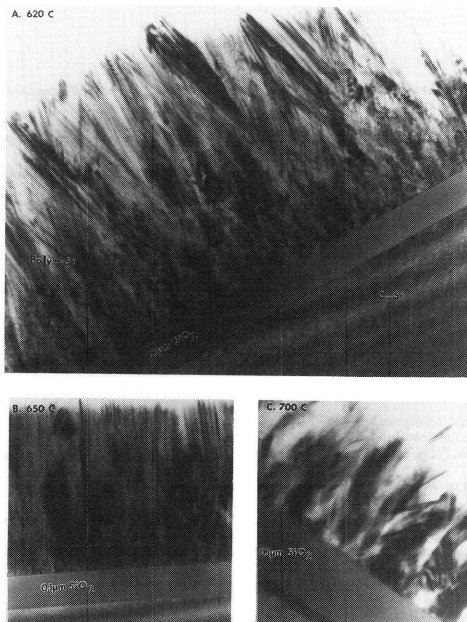


Figure 8. Stress profile of a compressive polysilicon film. The magnitude of stress is greatest at the  $\text{SiO}_2$  interface, explaining why thinner films exhibit greater compressive stress (see Figure 8).

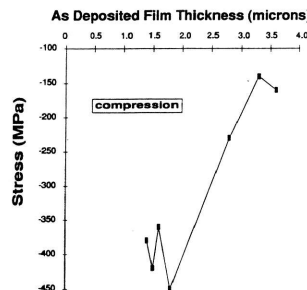
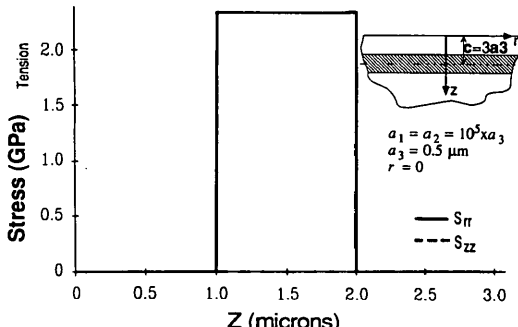


Figure 9. Average in-plane film stress vs. as-deposited film thickness for seven runs at 650°C. Thinner films have greater compressive stress.

Figure 7. Cross-sectional TEM micrographs of compressive films deposited at (A) 620°C, (B) 650°C, and (C) 700°C. Columnar grains grow out of a transition layer of small grains at the  $\text{SiO}_2$  interface. The thickness of the transition layer decreases with increasing temperature.



transformation strain to [21]

$$\epsilon^* = (\alpha_{film} - \alpha_{substr.})\Delta T = (3.3 \times 10^{-6} / ^\circ C - 3.7 \times 10^{-6} / ^\circ C)(605^\circ C) = .024\% \quad (5)$$

In this case,  $\sigma_{rr}$  is 56 MPa in the "film", and negligible in the "substrate". The thermal stress is thus insignificant compared to the observed stresses. Another example appears in Fig. 10, showing the stress distribution for an ellipse similar to the previous example, but buried one ellipse thickness below the surface of the substrate. This situation models two films on top of a substrate, with the bottom film having a different expansion coefficient than the top film and the substrate. Fig. 10 shows that  $\sigma_{rr}$  is only significant in the bottom "film", and negligible elsewhere, while  $\sigma_{zz}$  is negligible everywhere.

#### ACKNOWLEDGEMENTS

We are grateful to Jiahua Huang for her exceptionally careful experimental work and other contributions to the project. Thanks also to Tai D. Nguyen and Ron Gronsky for the original TEM work and valuable discussions. Conversations with Bob Ried, Rowland Cannon, Ali Imam, and Mauro Ferrari helped considerably with the development of the stress model. This research was funded by the Berkeley Sensor & Actuator Center, an NSF/Industry/University cooperative research center.

#### REFERENCES

1. R.I. Pratt, G.C. Johnson, and R.T. Howe, "Micromechanical Structures for Thin Film Characterization," *Digest of Technical Papers, Transducers '91, San Francisco, CA*, p. 205, June, 1991.
2. Bob Ried, private communication.
3. K. Seo and T. Mura, "The Elastic Field in a Half Space Due to Ellipsoidal Inclusions With Uniform Dilatational Eigenstrains," *J. Appl. Mech.*, vol. 46, p. 568, 1979.
4. J. Huang, P. Krulevitch, G.C. Johnson, R.T. Howe, and H.R. Wenk, "Investigation of Texture and Stress in Undoped Polysilicon Films," *Mat. Res. Soc. Symp. Proc.*, vol. 182, p. 201, 1990.
5. P. Krulevitch, R.T. Howe, G.C. Johnson, and J. Huang, "Stress in Undoped LPCVD Polycrystalline Silicon," *Digest of Technical Papers, Transducers '91, San Francisco, CA*, p. 949, June, 1991.
6. G.G. Stoney, "The Tension of Metallic Films Deposited by Electrolysis," *Proc. Roy. Soc. London*, vol. 9, p. 172, 1909.
7. Tai D. Nguyen, R. Gronsky, and J.B. Kontricht, "Cross-sectional Transmission Electron Microscopy of Multilayer Thin Film Structures," (*submitted to Journal of electron Microscopy Techniques*), 1990.
8. J. Magarino, D. Kaplan, R. Bisaro, J.F. Morhange, and K. Zelma, "Structural and Electronic Properties of CVD Silicon Films Near the Crystallization Temperature," *Journal de Physique*, vol. 43, pp. c1-271, 1982.
9. E. Kinsbrun, M. Sternheim, and R. Knoell, "Crystallization of Amorphous Silicon Films During Low Pressure Chemical Vapor Deposition," *Appl. Phys. Lett.*, vol. 42, p. 835, 1983.
10. J. Bloemberg and A.M. Beers, "In Situ Observations on Amorphous Versus Crystalline Growth of Silicon by Chemical Vapor Deposition," *Thin Solid Films*, vol. 124, p. 93, 1985.
11. H. Guckel, D.W. Burns, C.C.G. Visser, H.A.C. Tilmans, and D. DeRoo, "Fine-Grained Polysilicon Films with Built-In tensile Strain," *IEEE Trans. Electron Devices*, vol. ED-35, p. 800, 1988.
12. R.T. Howe and R.S. Muller, "Stress in Polycrystalline and Amorphous Silicon Thin Films," *J. Appl. Phys.*, vol. 54, p. 4674, 1983.
13. R.D. Mindlin and D.H. Cheng, "Thermoclastic Stress in the Semi-Infinite Solid," *J. Appl. Phys.*, vol. 21, p. 931, 1950.
14. M. Janai, D.D. Allred, D.C. Booth, and B.O. Seraphin, "Optical Properties and Structure of Amorphous Silicon Films Prepared by CVD," *Solar Energy Materials*, vol. 1, p. 11, 1979.
15. J.D. Eshelby, "The Determination of the Elastic Field of an Ellipsoidal Inclusion, and Related Problems," *Proceedings of the Royal Society, London*, vol. A, No. 241, p. 376, 1957.
16. P. Krulevitch, Tai D. Nguyen, G.C. Johnson, R.T. Howe, H.R. Wenk, and R. Gronsky, "LPCVD Polycrystalline Silicon Thin Films: The Evolution of Structure, Texture, and Stress," *Mat. Res. Soc. Symp. Proc.*, vol. 202, p. 167, 1990.
17. A. van der Drift, "Evolutionary Selection, A Principle Governing Growth Orientation in Vapour-Deposited Layers," *Philips Res. Repts.*, vol. 22, p. 267, 1967.
18. F.M. d'Heurle and J.M.E. Harper, "Note on the Origin of Intrinsic Stresses in Films Deposited Via Evaporation and Sputtering," *Thin Solid Films*, vol. 171, p. 81, 1989.
19. M.H. Brodsky, D. Kaplan, and J.F. Ziegler, "Densities of Amorphous Si Films by Nuclear Backscattering," *Appl. Phys. Lett.*, vol. 21, p. 305, 1972.
20. A. Lapicciarella, N. Tomassini, K.W. Lodge, and S.L. Altmann, "Force Field Treatment of an Amorphous Silicon Model," *Journal of Non-Crystalline Solids*, vol. 63, p. 301, 1984.
21. T. Suzuki, A. Mimura, and T. Ogawa, "The Deformation of Polycrystalline Silicon Deposited on Oxide-Covered Single Crystal Silicon Substrates," *J. Electrochem. Soc.*, vol. 124, p. 1776, 1977.

Figure 10.  $\sigma_{rr}$  and  $\sigma_{zz}$  vs. depth for a disc-shaped inclusion buried one disc thickness below the half space surface. The problem models stress in two films on a substrate in which the bottom film contracts.